Multiphase flowrate measurement with multi-modal sensors and temporal convolutional network

Multiphase flowrate measurement with multi-modal sensors and temporal convolutional network

Haokun Wang, *Student Member, IEEE*, Delin Hu, *Student Member, IEEE*, Maomao Zhang, *Member, IEEE*, Nan Li, *Member, IEEE*, and Yunjie Yang, *Member, IEEE*

***Abstract*— Accurate multiphase flow measurement is vital in monitoring and optimizing various production processes. Deep learning has as of late arose as a promising approach for assessing multiphase flowrate dependent on various customary flow meters. In this paper, we propose a multi-modal sensor and Temporal Convolution Network (TCN) based method to predict the volumetric flowrate of oil/gas two-phase flows. The volumetric flowrates of the liquid and gas phase vary from 0.96 - 6.13 m^3/h and 5.5 - 121.2 m^3/h, respectively. The multi-modal sequential sensing data are simultaneously collected from a Venturi tube and a dual-plane Electrical Capacitance Tomography (ECT) sensor in a pilot-scale multiphase phase flow facility. The reference data are derived from the single-phase flowmeters. Z-score and First-Difference (FD) data pre-processing methods are employed to manipulate the collected instantaneous time series multi-modal sensing data. The pre-processed data are utilized for training the TCN model. Experimental results reveal that the TCN model can effectively predict the multiphase flowrate based on the multi-modal sensing data.The results provide guidance on data pre-processing methods for multiphase flowrate estimation and demonstrate the effectiveness of combining multi-modal sensors and TCN for multiphase flowrate prediction under complex flow conditions.**

***Index Terms*— Temporal Convolutional Network (TCN), Z-score, first difference method, multiphase flowrate measurement, time series data.**

I. Introduction

MULTIPHASE flow refers to the simultaneous flow of two or more materials, frequently observed in the energy industry, chemical engineering, bio-medicine and natural environment. A growing body of literature recognizes the importance of accurate and in-situ multiphase flow measurement in real applications, which facilitates the improvement of production efficiency and safety, and reduces environmental pollution. In past decades, an assortment of multiphase flow measurement methods has been developed, which could be generally categorized into three distinct classes: multiphase flow visualization [1], flow pattern recognition [2], and flowrate measurement [3]. Each class involves notable attempts with the application of multiphase flow theory and the implementation of various measurement principles. Among these achievements, tomographic methods that are based on ultrasound [4], radiation [5], magnetic induction [6] and electrical field [7] are well established for multiphase flow measurement. The differential-pressure-based flow meters also play a non-negligible role in flow measurement, especially flowrate measurement [8].

Manuscript received ...

H. Wang, D. Hu and Y. Yang are with the SMART Group, School of Engineering, The University of Edinburgh, Edinburgh, UK, EH9 3FG. Corresponding author: Y. Yang (e-mail: y.yang@ed.ac.uk).

M. Zhang is with Tsinghua Shenzhen International Graduate School, Shenzhen, China, 77005 (e-mail: zhangmaomao@sz.tsinghua.edu.cn).

N. Li is with AIMCNT, School of Automation, Northwestern Polytechnical University, Xi'an, China (e-mail: nan.li@nwpu.edu.cn).

Multiphase flowrate measurement in the past profoundly relies on the separation tank, which is an unavoidable consititution in the traditional transportation system in energy industry. Its working principle depends on the gravity that automatically stratifies the mixture within a period. After stratification, Single Phase Flow Meters (SPFMs) are employed to measure the single phase flowrate. There is a broad scope of gadgets that can be viewed as the likely contender for single flowrate estimation, such as sensors based on terahertz [9] and acoustic technologies [10]. Differential pressure sensors such as Venturi tube are broadly utilized in single phase flowrate measurement [11]. This kind of SPFM estimates flowrate based on differential pressure signals created by the liquid flowing through the sensor. However, the spatial and temporal cost of using separators are considerably high, which dramatically reduces the production efficiency in real applications. Meanwhile, under the offshore scenarios, there are limited spaces available for pipelines and separation tanks.

With the advancement of sensors and computational methods, enormous efforts have been made to overcome the detriments of traditional flowrate estimation approaches. For instance, gamma-ray technique is combined with Venturi tube for flowrate measurement when flow regimes are stable [12]; the development of ultrasonic technique for multiphase flowrate measurement is systematically reviewed in [13]; the relationship between the flow condition, Doppler shift of the frequency shift of the acoustic wave and flow velocity is investigated in [14]. Studies of employing the Venturi tube in multiphase flowrate measurement have also been reported re-

cently. Differential pressure usually changes more dramatically in gas-liquid flows than single-phase flows. A recent study presents a comprehensive appraisal of relationships between the measured differential pressure and flowrate for gas-liquid slug flow through Venturi tubes [15]; another study examines the performance of Venturi tube in measuring the flowrate of a wide range of gas-liquid flows [16]. Nevertheless, it is noteworthy that the 'over reading' phenomenon occurs when utilizing the Venturi tube to measure multiphase flowrates. Compared to single phase flows, multiphase flows with the same mass or volumetric flowrate usually incites prominent differential pressure due to the existence of the other phase [17]. There have been attempts to utilize multi-modal approaches to tackle the flowrate measurement challenge, whilst there are still remaining issues. A drawback of combining Venturi tube with the radioactive approaches lies in the expensive maintenance and potential radiation hazards [18]. Integrating with sensors with direct contact of the flow (e.g., Electrical Resistance Tomography (ERT)) is sensitive to the impurity in the flow [19]. The combination of ECT and Venturi tube has been initially investigated in [20]. However, the mass flowrate were predicted based on simplified physical models.

The flourishing of data-driven methods has likewise presented new options for multiphase flowrate estimation by empowering more correlated sensing data analysis [21], [22]. A qualitative study in [23] compared different modern machine learning methods on predicting the multiphase flowrate using the Venturi tube. By employing Venturi meter as the primary sensor to extract the flow characteristics, our previous work successfully predicted the flowrate of gas-liquid flow using Deep Neural Network, (CNN)-Long-Short Term Memory (LSTM) and Temporal Convolutional Network (TCN) [3], [24]. However, the flowrate measurement accuracy still have the potential to be improved by combining multi-modal sensors with advanced learning algorithms.

This paper proposes an approach for estimating the fluid and gas volumetric flowrate of oil-gas two-phase flow by combining multi-modal sensors, i.e., dual-plane ECT sensor and the Venturi tube, with TCN. The multiphase flow is characterized by multi-modal sequential sensing data collected from the dual-plane ECT and Venturi tube. Then, TCN is firstly introduced to fuse the time series sensing data and estimate the flowrate. The TCN model is trained, validated, and tested using in-situ flow measurement data collected from a pilot-scale multiphase flow facility. The performance of TCN is comprehensively evaluated, and the effect of different data pre-processing approaches is also discussed.

The novelty of this work lies in: 1) Development of a multi-modal method for multiphase flowrate measurement based on ECT and Venturi tube; 2) Investigation of the effect of different multi-modal data pre-processing methods on the flowrate estimation accuracy; 3) Development of revised TCN models to fuse multi-modal time series data and estimate multiphase flowrate. Compared with the traditional mixture separation method, the proposed method is not sensitive to flow patterns and is able to perform in-situ flowrate measurement. By ultilizing multi-modal sensor data, the flowrate prediction accuracy could be improved.

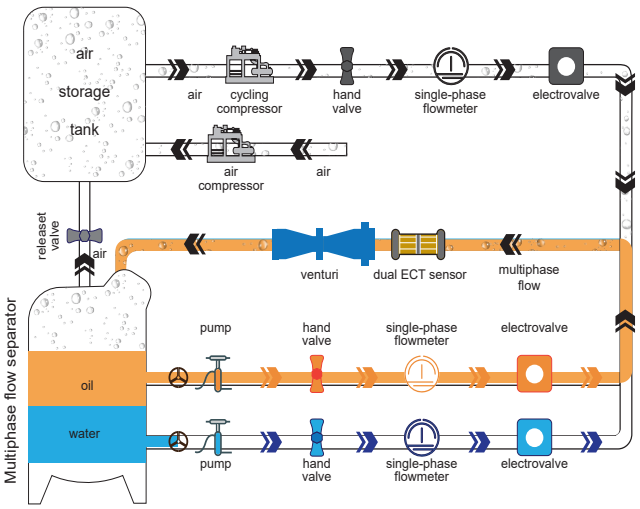

Fig. 1: Diagrammatic illustration of the multiphase flow facility for data collection.

II. Methods

A. Multiphase flow facility and data collection

The oil-gas two-phase flowrate measurement experiments were conducted on a pilot-scale multiphase flow facility (see Fig. 1 for schematic illustration). The multiphase flow facility comprises of an air storage tank, a separator to separate the mixture and supply the single phase flow of liquid, transport pipes, single phase flowmeters to provide reference flowrate of each phase, a Venturi tube to provide differential pressure data and a dual-plane 8-electrode ECT sensor to produce capacitance measurements. In the experiment, the flowrate of the oil and gas single phase flows is adjusted by solenoid valves to create an oil-gas mixture with various flow conditions. Meanwhile, the volumetric flowrate of each phase is measured through the Single-Phase Flow Meters (SPFMs) before mixing, which is adopted as the reference flowrate for the training of the machine learning model.

The oil and gas mixture is transported through the dual-plane ECT sensor and Venturi tube (see Fig. 2). The dual-plane ECT sensor is consisted of two layers of 8-electrode sensors. Each layer can provide 28 independent capacitance measurements, and in each measurement frame it can produce 28 * 2 capacitance readouts. The frame rate of the dual-plane ECT system is 714 fps [25]. Previous studies have demonstrated that the dual-plane sensor could capture velocity of the dispersed phase, which we expect will benefit flowrate estimation [26].

The mixture will then flow through the Venturi tube (see Fig. 2), which produces the differential pressure signal that correlates the flowrate of the multiphase flow. The structural design of the Venturi tube is based on several factors, such as the expected measurement range of multiphase flowrate and the working pressure of the facility. The throat diameter d is 25 mm and the diameter ratio is 0.5. The sampling frequency is 60 Hz and the resolution is 0.01 kPa. As illustrated in Fig. 2, three pressure signals namely the former (ΔP_f), posterior (ΔP_p) and dynamic pressure (P) are collected when the mixture flows

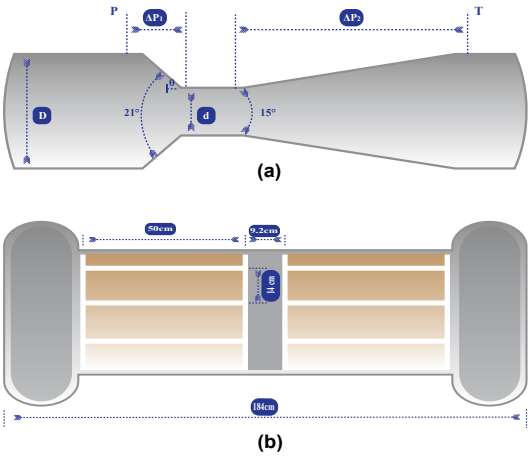

Fig. 2: Structural schematic of (a). the Venturi tube and (b). the dual-plane ECT sensor.

TABLE I: MULTIPHASE FLOW EXPERIMENT MATRIX

Objects	Liquid volumetric flowrate (m^3/h)	Gas volumetric flowrate (m^3/h)	GVF
Oil	0.96 – 6.13	-	-
Gas	-	5.5–121.2	0 – 96.64%

through it. Additionally, we measure the temperature (T) as an extra indication parameter for flowrate estimation.

B. Flow parameters measurement

We measure real-time capacitance from the dual-plane ECT sensor, differential pressure and temperature data from the Venturi tube according to the experimental matrix in Table. I. Considering the dynamic nature of the flow after mixing, we average the measured reference data from the SPFMs to more precisely approach the averaged multiphase flowrate in a short period. To simulate the flow conditions in real industrial applications, we perform a wide range control of each single phase flowrate during the experiment to cover the real situation in the production process as much as possible. The flowrate of the oil and gas phase ranges from 0.96-6.13 m^3/h and 5.5 - 121.2 m^3/h, respectively. The Gas Volume Fraction (GVF) varies from 0 to 96.94%.

The differential pressure, temperature and ECT data were considered in this study since the Venturi tube has been widely investigated for single-phase flowrate measurement, and the dual-plane ECT sensor has been proved effective in measuring the velocity of dispersed phases. The combination of Venturi tube and dual-plane ECT sensor is expected to improve the flowrate estimation accuracy for multiphase flows. With the sampling rate of 10 Hz, two differential pressure ΔP_f and ΔP_p, standard pressure and temperature data were simultaneously measured through Venturi tube and temperature sensors. Meanwhile, the dual ECT system with 8 electrodes on each plane concurrently acquires 56 capacitance measurements with 714 × 56 readings per second. Therefore, for a roughly half hour measurement duration, we initially obtain two 28*1285200 matrices for electrical parameters and four 1 * 15204 matrices for differential pressure and temperature parameters, which contain the instantaneous multiphase flow feature measurement results. In consideration of the consistency of the input training data feature to the proposed TCN model, the measured electrical parameters were averaged in each second to reflect the flow status during the one second period. Therefore, two 28 * 15204 electrical parameter matrices are obtained and considered as part of the final training data for TCN model. An overview of the instantaneous sequential pressure and temperature data is shown in Fig. 3. The temperature parameter stays at around 35°C and is represented by the purple colour. Meanwhile, the orange, yellow and blue dash lines indicate the measured pressure data to reflect the change in flow status.

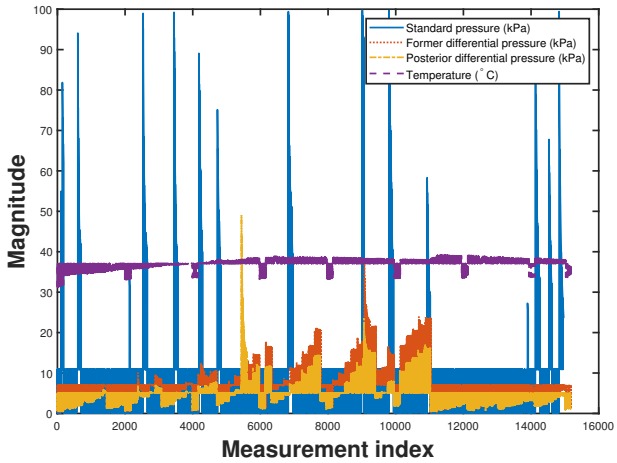

Fig. 3: Overview of the instantaneous pressure and temperature data.

C. Multi-modal data pre-processing

Data pre-processing on the instantaneous flow measurement data is essential to facilitate network training. It could eliminate to some extent the influence of measurement noise and achieve better alignment between the measurement and reference data. The difference of spatial locations of the sensors can cause a mismatch between the real instantaneous flowrate in the testing section and the flowrate calculated based on SPFM measurements, due to the dynamic nature of the multiphase flow. Our previous studies have proven that moving average is effective to mitigate this issue [3], [24]. On this basis, we further introduce two approaches for multi-modal data pre-processing.

1) Z-score method: Z-score, also known as zero-normalization, is one of the most popular data pre-processing (normalisation) methods in deep learning [27]. It is commonly applied to deal with features which have different scales to ensure the features are comparable with each other. The differential pressure, temperature and capacitance data are z-scored separately, and the z-score for each measurement is calculated by:

$$Z = \frac{x - \mu}{\sigma} \tag{1}$$

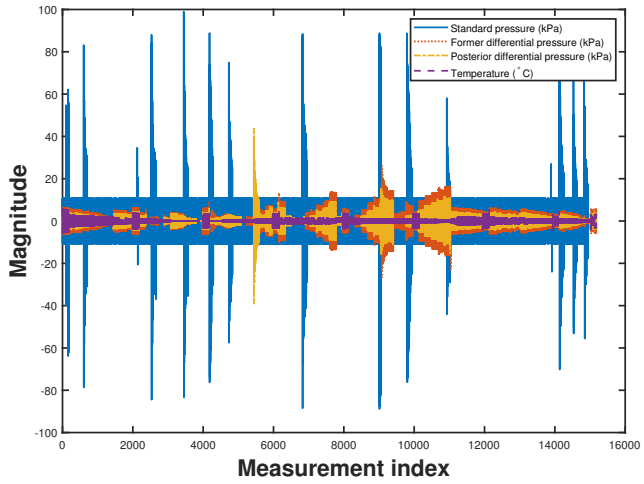

Fig. 4: Visualization of the first-difference pre-processed pressure and temperature training data.

where μ is the mean value; σ is the standard deviation and x is the measurement.

2) First-difference method: First-difference (FD) method is widely applied on dealing with sequential data in deep learning [28]. When the measurement data is sequentially collected and may be randomly varying, FD method is recommanded for data pre-processing. Meanwhile, implementing FD method to initially manipulate the raw data can avoid the stochastic trend problem [29]. The first difference method at time t can be defined as:

$$\Delta x_t = x_t - x_{(t-1)} \tag{2}$$

In this study, the FD was individually applied on each multiphase flow measurement and the pre-processed data is shown in Fig. 4. More smooth trend of both pressure and temperature data can be obtained after FD process.

D. TCN-based multiphase flowrate estimation

Notable progress has been made on the analysis and prediction of sequential data since the TCN model was proposed [30]. Our previous study implements an enhanced TCN to predict the multiphase flowrate using only Venturi tube [24]. Additionally, other learning-based methods such as 1D Convolutional Neural Network (CNN) [31], Deep Neural Network (DNN) and Support Vector Machine (SVM) [3] were attempted in our previous work. The vanishing/exploration gradient issue is evident, which could be addressed by TCN. This work further introduces a multi-modal setup and an improved TCN model to predict the multiphase flowrate based on multi-model data.

The TCN model in this work is established based on Keras library [32] and the main structure is illustrated in Fig. 5. Starting with the first layer, the batch size and input data length is respectively set to 32 and 128 for all six measured multiphase flow features. The measured P, ΔP_f, ΔP_p and T are 1D time-series signals. Therefore, an input format of 32*128*4 is adopted for the Venturi tube only case. Additionally, a 32*128*60 input configuration is created for the multi-modal setup integrating Venturi tube with the dual-plane ECT sensor, which introduces another 56 capacitance measurements.

A temporal block is directly connected to the input layer with its input dimension of (batch size * sequence length * channel), where the channel size is consistent with the input layer. It comprises eight independent TCNs with the same structure yet different parameter settings. A diagrammatic sketch of the temporal block is shown in Fig. 6.

The eight temporal blocks has the same parameter settings with the exception of the dilation ratio (d) and void rate (v), which are sequentially stated in the second block in Fig. 5. In detail, the parameter settings of the first temporal block on d and v are 1 and 0, respectively. With no special circumstances, it will not be repeated in the following text of this paper. The input data dimension of the temporal convolution block in Fig. 6 is consistent with previous network settings, where the channel size is selected as four for differential pressure and temperature features and 60 for electrical features obtained from dual ECT system. A convolution kernel is created in the 1D convolutional layer, which has the kernel size (k) of 2, zero padding size (p) of 2 and stride setting (s) of 1. The main function of the 1D convolutional layer is to perform the convolution operation with the input over a temporal dimension to generate outputs that contain a tensor. A normalization layer is followed with the conv 1D layer to perform the normalisation operation to avoid Internal Covariate Shift problem [33]. Layer Normalisation (LN) is then connected since it can analyze the input data of the same layer with different dimensions. As an improvement of Batch Normalisation (BN) method, the influence caused by the distribution of the mini-batch can be mitigated by implementing LN method. Meanwhile, compare to BN method, there is no need for LN to memorise the average and variance value of the mini-batch, which saves storage space during calculation. Due to the intrinsic characteristic of TCN, it can only "look forward" but not backward, zero padding operation will extend the size of the back. Therefore, a Chomp1D layer is connected to perform the "cutting" operation. In other words, the extended size of the back as the length of zero padding will be erased by the Chomp1d layer. Rectified Linear Unit function is selected as the activation function to eliminate the vanishing gradient problem in this study. For the temporal block, the structure of Conv 1D to Relu layer was repeated twice and the final dropout layer of a single TCN block provides an output (X_i) with the size of batch * 256.

The final dropout of the second block in Fig. 5 is achieved by performing the skip-layer connection operation of the eight TCNs' last layer of the temporal convolution block in Fig. 6. For eight temporal convolution blocks with the same structure, the output X_i is sequentially summarised, which can be noted as ($sum\{X_i\}$, where i = 1, 2 ... 8). Once the output of the temporal convolution block is obtained, two dense layers with 128 and 1 neurons are connected, which are the third and fifth layer in Fig. 6. The dense layer is essentially a fully connected layer, extracting the features obtained in temporal convolution layer and finding the relationships between these features. Adam [34] with the minimum training error was

Fig. 5: Schematic of TCN.

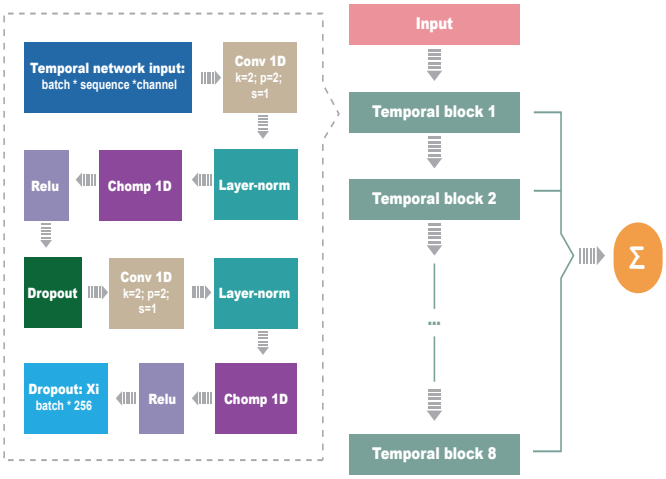

Fig. 6: Schematic of the temporal block in TCN.

chosen as the proper optimizer for current TCN model on solving the multiphase flowrate estimation problem.

The element of the TCN output (in Fig. 5) has the size of batch * 1, which is consistent with the format of the input data. It is one of the most obvious characteristics of the TCN model that it generates the same length of the output data with the input data. Data length consistency is achieved by implementing a 1D Fully Convolutional Network (FCN) architecture with zero padding operation. Another main characteristics of TCN is that there is no leakage of the information from the future to the past when implementing TCN to perform prediction objectives. It is benefited from the causal convolution architecture in the TCN model, which only conducts the convolution action with the elements at the current moment t and previous layers. Such capabilities enable us to flexibly control the output data length by adjusting the input data length.

E. Network parameters

For the TCN model in Fig 5 and 6, the parameters “k”, “p”, “s”, “d” and “v” denote the kernel size, zero padding, stride setting, dilation ratio and void rate, respectively. The kernel size was chosen as 2 according to [30]; the zero padding size is selected as 2 to ensure that the feature size remain unchanged after convolution operation; trade-off of the stride size need to be carefully considered, where small stride size enables avoiding repeat calculation and low training efficiency but large size may lead the lost of information and missing of key features of the training data. Therefore, the stride was set to 1 for best prediction results. The dilation ratio and void rate settings of each layer have been sequentially demonstrated. The Rectified Linear Unit (ReLU) function [35] was chosen as the activation function to eliminate and overcome the vanishing gradient problem.

We adopt the Mean Square Error (MSE) as the loss function, which calculates the squared difference between the estimated ($\hat{y}_i$) and reference (y_i) results:

$$J_{MSE} = \frac{1}{N}\sum_{i=1}^{N}[\hat{y}_i - y_i]^2 \tag{3}$$

where N is the number of the tested samples.

III. Results and Discussion

A. Network training

Section II-B states the collected training features. The multi-modal setup, i.e., the Venturi tube and dual-plane ECT system, generates differential pressure, temperature and capacitance data as training features. The flowrate measured by SPFMs before mixing is adopted to derive the true flowrate for network training. Two different data pre-processing methods are considered which are presented in Section II-C. Both pre-processing methods generate 15204 * 60 sequential samples, which contains 56 ECT features, 3 pressure features and 1 temperature feature. The training, validation and testing data set were randomly chosen from the sequential samples obtained with the ratio of 8:1:1. The epoch number was selected as 30 for TCN models, which has the lowest validation error. For Keras library, the value of the parameter Adam was set as 1e-3.

B. Results using Z-score pre-processing

Fig. 7 first shows the results based on z-score pre-processed features without including measurements from dual-plane ECT for comparison. Fig. 8 presents the results under the multi-modal setup, i.e., the instantaneous dual-plane ECT signals with the pressure and temperature features are utilised for the training of the proposed TCN model.

By contrasting various multiphase flow feature combinations for flowrate estimation, the results demonstrate a strong correlation between the estimated volumetric flowrate of the liquid/gas phase and the reference flowrate (see Fig.7 and 8). Most liquid and gas phase estimation results are located within the acceptable accuracy range. Statistically, when ECT data were not included in training, there are 86.49% and 75.55% estimation results are in the tolerable scope for the liquid and gas phase, respectively, suggesting the effectiveness of TCN on multiphase flowrate prediction. By further including ECT data, the TCN model demonstrates more precise results in Fig. 8. There are 89.68% and 93.83% results sitting within the tolerance range, indicating a considerable improvement. Especially for gas phase, including ECT data leads to 24.2%

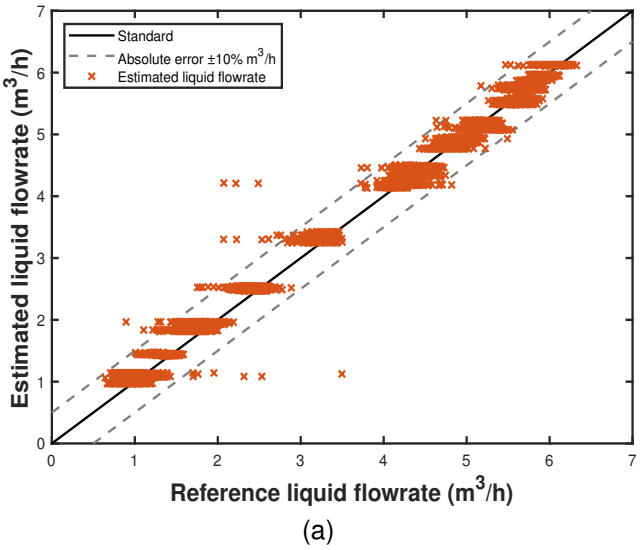

Fig. 7: Multiphase flowrate estimation results of (a) liquid phase and (b) gas phase by using TCN and Z-score pre-processing without dual-plane ECT data.

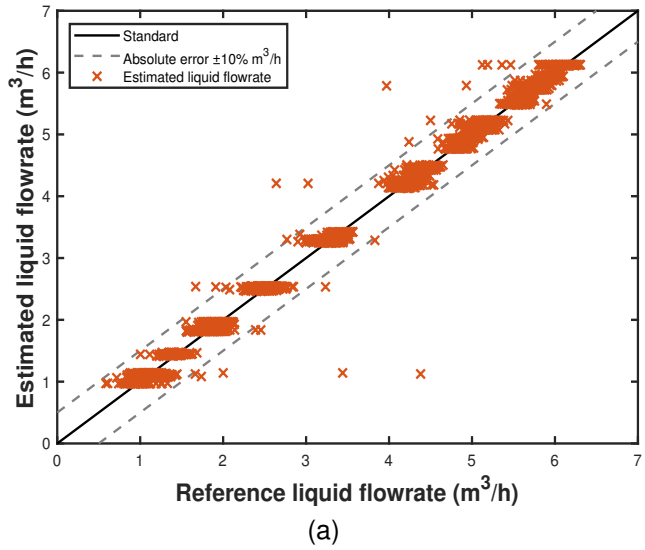

Fig. 8: Multiphase flowrate estimation results of (a) liquid phase and (b) gas phase by using TCN with Z-score pre-processing and dual-plane ECT data.

improvement. Compared with Fig.7, it shows that adding more proper multiphase flow features can increase the flowrate measurement accuracy.

In addition to the difference caused by training features, the estimated multiphase flowrate may also influenced by different phase (i.e. liquid and gas phase). Several outliers appear on the liquid phase in both Fig. 7a and 8a. There are three possible underlying reasons for less outliers in the gas phase shown in Fig. 7b and 8b. A possible explanation might be that the Venturi tube is more sensitive to wet gas measurement, leading to stronger linearity for the predicted gas flowrate. Another potential reason is that TCN model has intrinsic limitations on liquid phase flowrate prediction. In other words, TCN model may not be able to extract high dimension features on estimating the flowrate of the liquid phase.

The deviation of the estimation results (see Fig. 9) also echos the previous analysis. Most liquid and gas flowrates are within an acceptable range, while results based on four multiphase flow features demonstrate a relatively larger deviation. Meanwhile, more outliers also appear in results using fewer features. The deviation plots further confirm the ability of TCN on multiphase flowrate estimation with proper training data. Additionally, the benefit of introducing dual-plane ECT data is also validated.

C. Results using first-difference pre-processing

The FD pre-processing method was also applied on the collected multiphase flow features and the TCN model was trained separately by different feature combinations. The flowrate estimation results are shown in Fig. 10 and 11.

Observing both figures, the number of outliers are reduced considerably. The stronger linearity between the estimated and reference flowrate could be attributed to the characteristic of FD pre-processing method, which has been widely applied

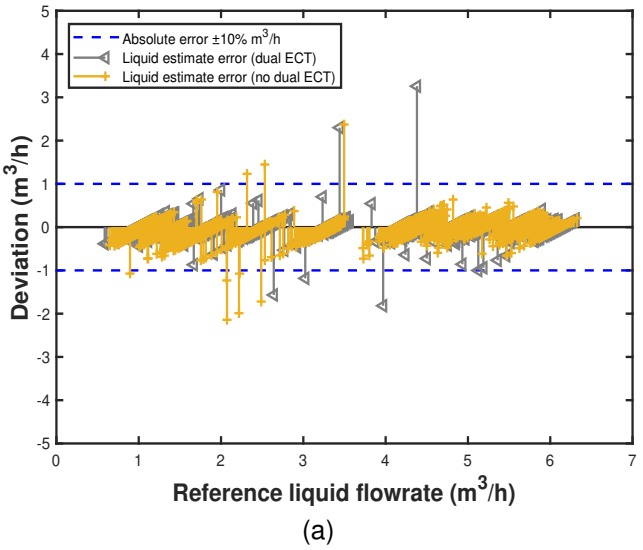

Fig. 9: Deviation of (a) liquid phase and (b) gas phase estimations with and without dual-plane ECT data by implementing Z-score pre-processing method.

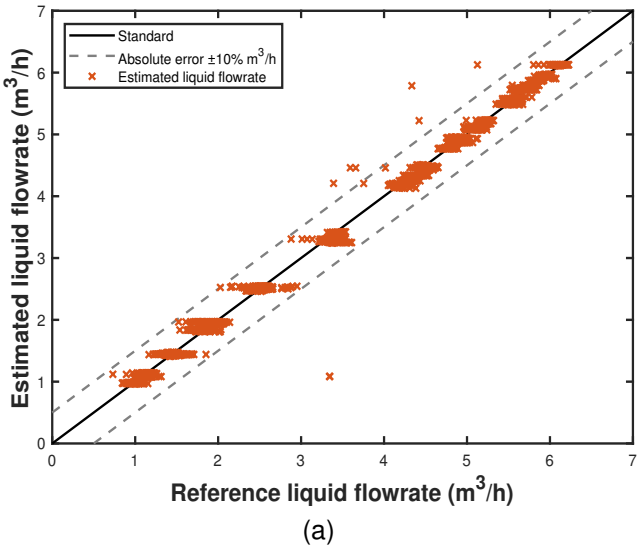

Fig. 10: Multiphase flowrate estimation results of (a) liquid phase and (b) gas phase using TCN with FD pre-processing without dual-plane ECT data.

on dealing with unstable sequential data. The effect of the dual-plane ECT data on estimation accuracy is also reflected in both figures. When electrical signals are not included in training, there are 90.64% and 85.14% of the predicted flowrates within the 10% range for liquid and gas phases, respectively. A comprehensive training data set which contains 56 groups of ECT data increases the valid predicted flowrate to 95.84% and 98.3% for liquid and gas phases, respectively. This corroborates the earlier findings that the prediction accuracy can be significantly improved by including extra multiphase flow characteristics in the training process.

Fig. 12 shows the corresponding deviation distribution of the estimated flowrates. The improvement of the estimation accuracy is apparent when comprehensive training data is utilized. A clearer linearity between the estimated and reference flowrates exists when the dual-plane ECT data is used as extra training data.

D. Comparison between Z-score and FD methods

Based on the predicted flowrate shown in Section III-B and III-C, the performance of the TCN model and the influence of different data pre-processing methods will be qualitatively and quantitatively evaluated in horizontal (comparison of the calculated MSE and $\rho_{X,Y}$) and longitudinal (different data pre-processing) perspective. The quantitative evaluation of the predicted flowrate is mainly based on MSE and linear correlation index ($\rho_{X,Y}$). The latter describes the correlation between the dependent and independent variables, which is expressed as:

$$\rho_{X,Y} = \frac{E[(X - E(X))(Y - E(Y))]}{\sqrt{E[X - E(X)]^2}\sqrt{E[Y - E(Y)]^2}} \tag{4}$$

where E stands for expectation operation, X and Y represents the estimated and reference multiphase flowrate, respectively.

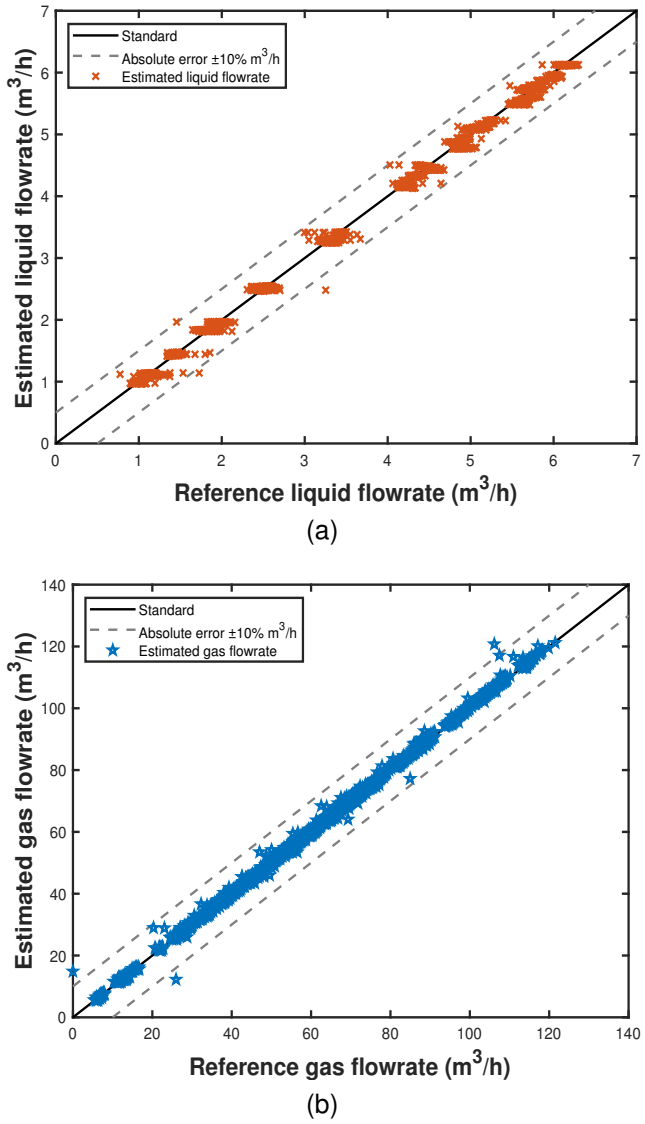

Fig. 11: Multiphase flowrate estimation results of (a) liquid phase and (b) gas phase using TCN with FD pre-processing with dual-plane ECT data.

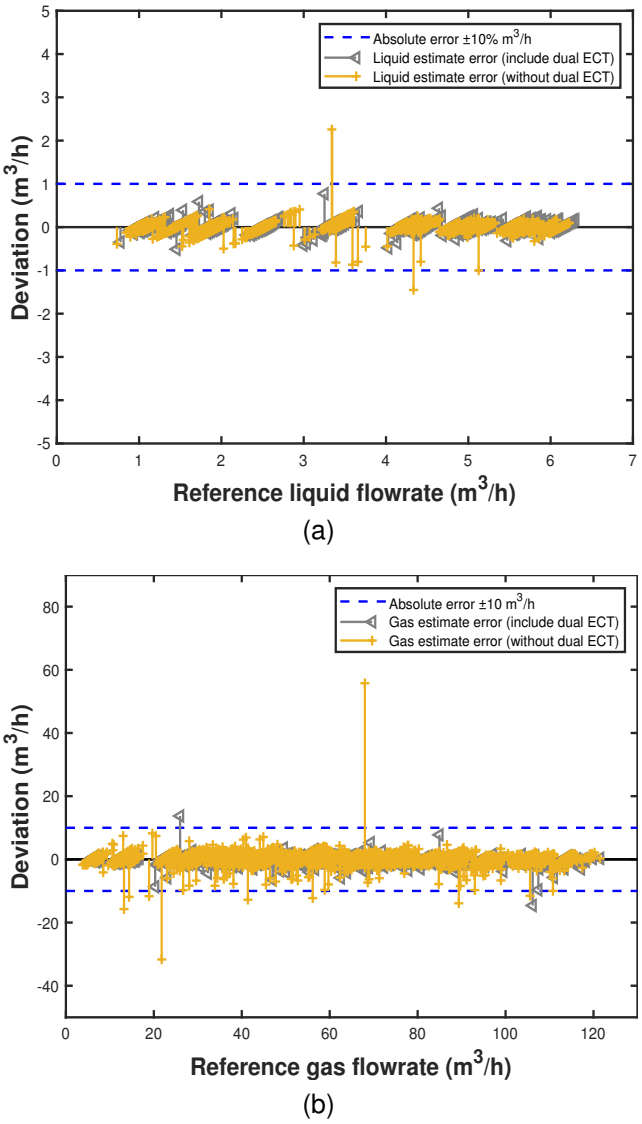

Fig. 12: Deviation of (a) liquid phase and (b) gas phase using TCN with and without dual-plane ECT data by implementing FD pre-processing.

The closer the absolute value of $\rho_{X,Y}$ is to 1, the stronger the linear relationship.

Table. II provides the MSE and $\rho_{X,Y}$ obtained from the preliminary analysis of the estimated multiphase flowrate. What stands out in the "Z-score" columns is that the smallest MSE and highest correlation index appears in Fig. 8a and 8b for the liquid and gas phase, respectively. Similar phenomenon can be observed in Fig. 11a and 11b when implementing FD method. This indicates that the estimation accuracy of the liquid and gas flowrates can be improved by including ECT data when training the TCN model. Meanwhile, for both data pre-processing methods, the estimated gas flowrate commonly has greater $\rho_{X,Y}$ and MSE value compared to the same group of the results on liquid phase. It is aware that stronger linearity does not necessarily correspond to a smaller MSE. Compared with the liquid phase, a higher MSE of the estimated gas flowrate is due to a wider acceptable range since it is still a challenge to accurately measure gas flowrate in energy industry.

Comparing each row, the TCN trained with FD pre-processed data is better than that with Z-score data with higher linear correlation index value and lower MSE. It could be due to that the intrinsic characteristic of the Z-score method, which excludes the consideration of the physical meaning of the multiphase flow characteristics rather than executing the data manipulation only from the perspective view of the data structure. Additionally, Fig. 11a and 11b reveal the best performance of the predicted liquid and gas flow of TCN model by including ECT data in training and implementing FD data pre-processing method. For the same training set and TCN model, we can also conclude that FD method outperforms Z-score method as the worst predicted results of FD method (Fig. 10a and 10b) is still better than the best of Z-score (Fig. 8a and 8b) with lower MSE and higher correlation index value.

TABLE II: CORRELATION INDEX AND MSE OF ESTIMATED FLOWRATE USING TCN WITH DIFFERENT DATA PRE-PROCESSING METHODS

Index[1]	Z-score		First difference	
	Liquid	Gas	Liquid	Gas
ρ_{-E}	0.9977 (Fig. 7a)	0.9992 (Fig. 7b)	0.9992 (Fig. 10a)	0.9994 (Fig. 10b)
ρ_{+E}	0.9990 (Fig. 8a)	0.9997 (Fig. 8b)	0.9997 (Fig. 11a)	0.9999 (Fig. 11b)
MSE_{-E}	0.0209 (Fig. 7a)	1.5369 (Fig. 7b)	0.0049 (Fig. 10a)	1.1625 (Fig. 10b)
MSE_{+E}	0.0064 (Fig. 8a)	0.5503 (Fig. 8b)	0.0024 (Fig. 11a)	0.2079 (Fig. 11b)

[1] The subscript "$-E$" and "$+E$" stands for the training data sets excluding and including dual-plane ECT data, respectively.

IV. CONCLUSION

This paper first introduced TCN for multiphase flowrate estimation based on the multi-modal setup and investigated the influence of different data pre-processing methods on estimation accuracy. The dual-plane ECT sensor was combined with the Venturi tube to obtain the multiphase flowrate features. Two different data pre-processing methods (Z-score and FD) were implemented to manipulate the obtained instantaneous time-series signals. The experiment results confirms the superior performance of TCN on estimating the multiphase flowrate. We also show that the dual-plane ECT data play a vital role in obtaining more accurate flowrates under the multi-modal setup. Another finding is that FD approach can provide more accurate flowrate estimation for both liquid and gas phases.

Future work can further investigate the generalization ability of the proposed approach under various experimental conditions and facilities.

REFERENCES

[1] A. T. Krummel, S. S. Datta, S. Münster, and D. A. Weitz, "Visualizing multiphase flow and trapped fluid configurations in a model three-dimensional porous medium," *AIChE Journal*, vol. 59, no. 3, pp. 1022–1029, 2013.

[2] Y. Yan, L. Wang, T. Wang, X. Wang, Y. Hu, and Q. Duan, "Application of soft computing techniques to multiphase flow measurement: A review," *Flow Measurement and Instrumentation*, vol. 60, pp. 30–43, 2018.

[3] H. Wang, M. Zhang, and Y. Yang, "Machine learning for multiphase flowrate estimation with time series sensing data," *Measurement: Sensors*, vol. 10, p. 100025, 2020.

[4] C. Tan, X. Li, H. Liu, and F. Dong, "An ultrasonic transmission/reflection tomography system for industrial multiphase flow imaging," *IEEE Transactions on Industrial Electronics*, vol. 66, no. 12, pp. 9539–9548, 2019.

[5] A. Bieberle, H. Nehring, R. Berger, M. Arlit, H.-U. Härting, M. Schubert, and U. Hampel, "Compact high-resolution gamma-ray computed tomography system for multiphase flow studies," *Review of Scientific Instruments*, vol. 84, no. 3, p. 033106, 2013.

[6] L. Ma and M. Soleimani, "Magnetic induction tomography methods and applications: A review," *Measurement Science and Technology*, vol. 28, no. 7, p. 072001, 2017.

[7] M. Zhang, L. Zhu, H. Wang, Y. Li, M. Soleimani, and Y. Yang, "Multiple measurement vector-based complex-valued multifrequency ect," *IEEE Transactions on Instrumentation and Measurement*, vol. 70, pp. 1–10, 2020.

[8] D. Bridgeman, F. Tsow, X. Xian, and E. Forzani, "A new differential pressure flow meter for measurement of human breath flow: Simulation and experimental investigation," *AIChE Journal*, vol. 62, no. 3, pp. 956–964, 2016.

[9] I. M. Saied, M. Meribout, E. Kato, and X. H. Zhao, "Terahertz spectroscopy for measuring multiphase fractions," *IEEE Transactions on Terahertz Science and Technology*, vol. 7, no. 3, pp. 250–259, 2017.

[10] M. Meribout, A. Al Naamany, and K. Al Busaidi, "An acoustic system for providing the two-phase liquid profile in oil field storage tanks," *IEEE transactions on ultrasonics, ferroelectrics, and frequency control*, vol. 56, no. 10, pp. 2241–2250, 2009.

[11] A. Skea and A. Hall, "Effects of gas leaks in oil flow on single-phase flowmeters," *Flow measurement and Instrumentation*, vol. 10, no. 3, pp. 145–150, 1999.

[12] Y. Ma, C. Li, Y. Pan, Y. Hao, S. Huang, Y. Cui, and W. Han, "A flow rate measurement method for horizontal oil-gas-water three-phase flows based on venturi meter, blind tee, and gamma-ray attenuation," *Flow Measurement and Instrumentation*, p. 101965, 2021.

[13] C. Tan, Y. Murai, W. Liu, Y. Tasaka, F. Dong, and Y. Takeda, "Ultrasonic doppler technique for application to multiphase flows: A review," *International Journal of Multiphase Flow*, p. 103811, 2021.

[14] X. Dong, C. Tan, Y. Yuan, and F. Dong, "Oil–water two-phase flow velocity measurement with continuous wave ultrasound doppler," *Chemical Engineering Science*, vol. 135, pp. 155–165, 2015.

[15] Y. Liu, Y. Deng, M. Zhang, P. Yu, and Y. Li, "Experimental measurement of oil–water two-phase flow by data fusion of electrical tomography sensors and venturi tube," *Measurement Science and Technology*, vol. 28, no. 9, p. 095301, 2017.

[16] A. Zeghloul, A. Messilem, N. Ghendour, A. Al-Sarkhi, A. Azzi, and A. Hasan, "Theoretical study and experimental measurement of the gas liquid two-phase flow through a vertical venturi meter," *Proceedings of the Institution of Mechanical Engineers, Part C: Journal of Mechanical Engineering Science*, vol. 235, no. 9, pp. 1567–1584, 2021.

[17] Y. Xu, Q. Zhang, T. Zhang, and X. Ba, "An overreading model for nonstandard venturi meters based on h correction factor," *Measurement*, vol. 61, pp. 100–106, 2015.

[18] Y. Pan, C. Li, Y. Ma, S. Huang, and D. Wang, "Gas flow rate measurement in low-quality multiphase flows using venturi and gamma ray," *Experimental Thermal and Fluid Science*, vol. 100, pp. 319–327, 2019.

[19] W. Chen, J. Li, Y. Li, M. Zhang, and L. Peng, "Flowrate estimation of horizontal gas–water slug flow based on venturi tube and conductance sensor," *IEEE Transactions on Instrumentation and Measurement*, vol. 70, pp. 1–10, 2021.

[20] Z. Huang, D. Xie, H. Zhang, and H. Li, "Gas–oil two-phase flow measurement using an electrical capacitance tomography system and a venturi meter," *Flow measurement and Instrumentation*, vol. 16, no. 2-3, pp. 177–182, 2005.

[21] D. Hu, J. Li, Y. Liu, and Y. Li, "Flow adversarial networks: Flowrate prediction for gas–liquid multiphase flows across different domains," *IEEE transactions on neural networks and learning systems*, vol. 31, no. 2, pp. 475–487, 2019.

[22] X. Lin, H. Wang, Z. Chen, H. Zhang, and Y. Li, "Measurement of the flow rate of oil and water using microwave and venturi sensors with end-to-end dual convolutional neural network," *Measurement: Sensors*, vol. 10, p. 100018, 2020.

[23] Z. Jiang, H. Wang, Y. Yang, and Y. Li, "Comparison of machine learning methods for multiphase flowrate prediction," in *2019 IEEE International Conference on Imaging Systems and Techniques (IST)*. IEEE, 2019, pp. 1–6.

[24] H. Wang, D. Hu, M. Zhang, and Y. Yang, "Multiphase flowrate measurement with time series sensing data and sequential model," *International Journal of Multiphase Flow*, p. 103875, 2021.

[25] Y. Yang, L. Peng, and J. Jia, "A novel multi-electrode sensing strategy for electrical capacitance tomography with ultra-low dynamic range," *Flow Measurement and instrumentation*, vol. 53, pp. 67–79, 2017.

[26] S. Sun, X. Lu, L. Xu, Z. Cao, J. Sun, and W. Yang, "Real-time 3-d imaging and velocity measurement of two-phase flow using a twin-plane

ect sensor," *IEEE Transactions on Instrumentation and Measurement*, vol. 70, pp. 1–10, 2021.
[27] S. Patro and K. K. Sahu, "Normalization: A preprocessing stage," *arXiv preprint arXiv:1503.06462*, 2015.
[28] J. Wang, W. Tu, L. C. Hui, S.-M. Yiu, and E. K. Wang, "Detecting time synchronization attacks in cyber-physical systems with machine learning techniques," in *2017 IEEE 37th International Conference on Distributed Computing Systems (ICDCS)*. IEEE, 2017, pp. 2246–2251.
[29] T. Stadnytska, "Deterministic or stochastic trend," *Methodology*, 2010.
[30] S. Bai, J. Z. Kolter, and V. Koltun, "An empirical evaluation of generic convolutional and recurrent networks for sequence modeling," *arXiv preprint arXiv:1803.01271*, 2018.
[31] H. Zhang, Y. Yang, M. Yang, L. Min, Y. Li, and X. Zheng, "A novel cnn modeling algorithm for the instantaneous flow rate measurement of gas-liquid multiphase flow," in *Proceedings of the 2020 12th International Conference on Machine Learning and Computing*, 2020, pp. 182–187.
[32] T. B. Arnold, "kerasr: R interface to the keras deep learning library," *Journal of Open Source Software*, vol. 2, no. 14, p. 296, 2017.
[33] D. Arpit, Y. Zhou, B. Kota, and V. Govindaraju, "Normalization propagation: A parametric technique for removing internal covariate shift in deep networks," in *International Conference on Machine Learning*. PMLR, 2016, pp. 1168–1176.
[34] N. Ketkar, "Introduction to keras," in *Deep learning with Python*. Springer, 2017, pp. 97–111.
[35] A. F. Agarap, "Deep learning using rectified linear units (relu)," *arXiv preprint arXiv:1803.08375*, 2018.